Journal of Organometallic Chemistry, 378 (1989) 473–483
Elsevier Sequoia S.A., Lausanne – Printed in The Netherlands
JOM 20350

The syntheses, structures and stereodynamics of [3]ferrocenophane complexes

II *. Trimethylplatinum(IV) halide complexes, $[PtXMe_3\{(C_5H_4ECH_3)_2Fe\}]$ (E = S, Se; X = Cl, Br, I)

Edward W. Abel, Nicholas J. Long, Keith G. Orrell, Anthony G. Osborne, and Vladimir Šik

Department of Chemistry, The University, Exeter, EX4 4QD (Great Britain)

(Received March 16th, 1989)

Abstract

The syntheses of the complexes $[PtXMe_3\{(C_5H_4ECH_3)_2Fe\}]$ (E = S, Se; X = Cl, Br, I) are reported. A variable temperature NMR study of their solution properties revealed varying rates of pyramidal inversion of the coordinated chalcogen atoms. When inversion is slow on the ^1H or ^{195}Pt NMR time-scales, the DL forms of the complex predominate ($\geq 90\%$ abundance). Activation energies ($\Delta G^{\ddagger}$(298 K)/kJ mol^{-1}) for the pyramidal inversions fall in the narrow ranges 41.7–43.4 (sulphur) and 58.0–58.8 (selenium). At above-ambient temperatures averaging of the ring proton NMR signals indicates that the ligand is executing 180° 'pancake' rotations with respect to the trimethylplatinum(IV) halide moiety, accompanied by exchange of the Pt-methyl environments. The NMR spectra also imply that the E–Pt–E portion of the ring is rapidly moving from one half-chair form to the other at all observed temperatures.

Introduction

As part of a wide-ranging study on the intramolecular motions of chalcogen-containing molecules coordinated to a transition metal, we have synthesised and carried out detailed dynamic NMR studies of a considerable number of complexes derived from the trimethylplatinum(IV) halides. These studies have led to the identification of some novel intramolecular rearrangements and the measurement of their energy barriers [1,2].

* For part I see ref. 3.

0022-328X/89/$03.50

We have now commenced a study of the metal complexes formed by the organometallic ligands 1,1′-bis(methylthio)ferrocene (BMSF) and 1,1′-bis(methylseleno)ferrocene (BMSEF). We recently reported [1] synthetic and spectroscopic studies on the complexes formed by these ligands with the Group 6 tetracarbonyl moieties. We now report the syntheses and NMR characterisation of the solution stereodynamics of the complexes *fac*-[$PtXMe_3$(BMSF)] and *fac*-[$PtXMe_3$(BMSEF)] (X = Cl, Br, I), the principal aims of the work being to compare the preferred solution species and the energies of the fluxions present in these pseudo-six-membered ferrocenophane complexes with those pertaining to the analogous complexes of six-membered dithio- and diseleno-ether ligands, $MeE(CH_2)_3EMe$ (E = S, Se) [1,2].

Experimental

General

All preparations were carried out by standard Schlenk techniques [4]. All reactions were performed under purified nitrogen using freshly distilled, dried, and degassed solvents.

The following compounds were prepared by published methods; [$(PtXMe_3)_4$] (X = Cl, Br, I) [5–7], 1,1′-bis(methylthio)ferrocene (BMSF) [8], 1,1′-bis(methylseleno)ferrocene (BMSEF) [3].

Elemental analyses were performed by Butterworth Laboratories Ltd., Teddington, Middlesex, London and by C.H.N. Analysis, South Wigston, Leicester.

Synthesis of complexes

All the complexes were prepared in a similar fashion. A typical example is outlined below, and details of all the synthetic and analytical data are summarised in Table 1.

Table 1

Synthetic, melting temperature and analytical data for the complexes [$PtXMe_3$(L–L)] (X = Cl, Br, I; L–L = chelating ferrocenylchalcogenide)

Complex	Reaction time (h)	Yield [a] (%)	Melting temperature (°C)	Analytical Data (Found (calc)(%))	
				C	H
[$PtClMe_3$(BMSF)] (1)	6	81	180–190d	32.5 (32.5)	4.2 (4.2)
[$PtBrMe_3$(BMSF)] (2)	6	88	180–190d	30.1 (30.1)	3.9 (3.9)
[$PtIMe_3$(BMSF)] (3)	6	68	180–190d	27.6 (27.9)	3.5 (3.6)
[$PtClMe_3$(BMSEF)] (4)	16	55	142–144	27.8 (27.8)	3.7 (3.6)
[$PtBrMe_3$(BMSEF)] (5)	16	40	165–167	26.3 (26.0)	3.4 (3.3)
[$PtIMe_3$(BMSEF)] (6)	16	37	151–153	24.6 (24.4)	3.2 (3.1)

[a] Yield quoted relative to the $PtXMe_3$ monomeric unit. d = decomposition.

$[(PtBrMe_3)_4]$ (0.352 g, 1.1 mmol, based on the monomeric unit) was dissolved in benzene (20 cm^3). BMSF (0.40 g, 1.44 mmol) in benzene (20 cm^3) was added, and the solution was stirred and refluxed for 6 h to produce an orange-brown solution. This was filtered and evaporated to dryness under reduced pressure. The residual solid was washed with hexane (2×20 cm^3) and recrystallised from dichloromethane/hexane (1/1) to produce orange crystals of *fac*-$[PtBrMe_3(BMSF)]$. Yield 0.58 g (88%).

NMR studies

^1H, $^{13}C\{^1H\}$ and $^{195}Pt\{^1H\}$ NMR spectra were recorded on a Bruker AM250 FT spectrometer, operating at 250.13, 62.90 and 53.53 MHz, respectively.

All spectra were recorded as $CDCl_3$ or CD_2Cl_2 solutions. ^1H and ^{13}C chemical shifts are quoted relative to Me_4Si as internal standard, whilst ^{195}Pt chemical shifts are quoted relative to Ξ (^{195}Pt) 21.4 MHz.

A standard B-VT1000 variable temperature unit was used to control the probe temperature; the calibration of this unit was checked periodically against a Comark digital thermometer. The temperatures are considered accurate to $\pm 1°C$. Band-shape analyses were performed by use of modified versions of the program DNMR devised by Kleier and Binsch [9,10].

Results and discussion

Static NMR measurements

At the limiting low temperatures studied, the proton spectra of all the complexes revealed a single predominant solution species with a trace of a second species. Static ^1H chemical shift and spin–spin coupling constant data are given in Table 2 (BMSF complexes) and Table 3 (BMSEF complexes). The pairs of strong E-methyl signals are invariably of exactly equal intensity, implying that the predominant species are DL forms with the E-methyls in a mutual *anti*-relationship which renders them anisochronous. The very weak additional signals are compatible with a *meso* structure in which the E-methyls are equivalent. The relative populations of the two solution species were most clearly measured from the ^{195}Pt NMR spectra of the complexes. The data for all six complexes are contained in Table 4. It will be noted that the DL signal is always to lower frequency of the weak *meso* signal and its assignment is unambiguously confirmed in the case of the BMSEF complexes by the presence of two pairs of ^{77}Se satellites from the different magnitudes of ^{195}Pt couplings to the non-equivalent Se atoms in the DL species. The case of $[PtClMe_3(BMSEF)]$ is illustrated in Fig. 1. where the $^1J(PtSe)$ values are 231 and 339 Hz.

Dynamic NMR measurements

On raising the temperature of the NMR samples, exchange broadening was observed in the proton spectra (see later) indicating the onset of internal molecular motion(s). Two possible intramolecular rate processes may be the cause of these spectral changes, namely pyramidal inversion of the coordinated chalcogens, and reversal of the E–Pt–E portion of the ferrocenophane ring. If both processes are slow on the NMR timescale, then six NMR-distinguishable species are possible, namely four *meso* species, *meso*-**1**, **2**, **3** and **4**, and two mirror-image DL pairs, DL-**1**

Table 2

^{1}H NMR data for the complexes [PtXMe$_3$(BMSF)] in CD_2Cl_2 at low and ambient temperatures

Complex No.	X	Temperature (°C)	Invertomer	Chemical shift Pt–Me protons (δ)	Chemical shift S–Me protons (δ)	Chemical shift ring protons (δ) [a]	
1	Cl	−70	DL	1.11(t) [d]	2.57(t)	5.42	4.53
				1.04(2×t)	2.29(t)	4.40	4.22
			meso		2.64(t)	4.92	4.24
		20	DL/*meso*	1.18(t)[70.1] [b]	2.56(t)[12.6] [c]	5.10	4.45
				1.16(t)[71.1]		4.34	4.31
2	Br	−60	DL	1.21(t)[70.7] [b]	2.57(t)[13.9] [c]	5.50	4.52
				1.11(t)[69.1]	2.29(t)[14.1]	4.40	4.39
				1.08(t)[70.0]			
		20	DL/*meso*	1.27(t)[70.7] [b]	2.57(t)[13.1] [c]	5.13	4.46
				1.26(t)[70.3]		4.33	
3	I	−60	DL	1.37(t)[69.5] [b]	2.68(t)[14.5] [c]	5.61	4.53
				1.33(t)[69.9]	2.30(t)[14.3]	4.43	4.23
				1.22(t)[70.6]			
		0	DL/*meso*	1.42(t)[68.8] [b]	2.59(t)[13.9] [c]	5.18	4.51
				1.39(t)[70.6]		4.35	

[a] Signals show weak multiplet structure in most cases. [b] ^2J(PtH) (Hz) values. [c] ^3J(PtH) (Hz) values. [d] t = triplet.

and **2**. These species may be related by the eight corners of a cube (Fig. 2). Chalcogen inversion will inter-convert the four forms on the front face, and also those on the rear face of the cube, whereas bridge reversal will exchange adjacent

Table 3

^{1}H NMR parameters for the complexes [PtXMe$_3$(BMSEF)] in $CDCl_3$ at low and high temperatures

Complex No.	X	Temperature (°C)	Invertomer	Chemical shift Pt–Me protons (δ)	Chemical shift Se–Me protons (δ)	Chemical shift ring protons (δ) [a]	
4	Cl	−40	DL	1.17(t)[71.5] [b]	2.50(t)[10.8] [c]	5.39	4.48
				1.15(t)[69.3]	2.19(t)[11.6]	4.42	4.38
				1.14(t)[69.3]		4.27	4.24
			meso		2.57(t)[10.3] [c]		
		+50	DL/*meso*	1.28(t)		5.04	4.38
				1.18(t)	2.44(t)[9.9] [c]	4.31	
5	Br	−40	DL	1.28(t)[71.2] [b]	2.56(t)[11.1] [c]	5.47	4.48
				1.26(t)[68.7]	2.19(t)[11.6]	4.43	4.39
				1.21(t)[69.3]		4.29	4.26
			meso		2.63 [d]		
		+50	DL/*meso*	1.34(t)		5.08	4.38
				1.27(t)	2.41 [e]	4.29	
6	I	−40	DL	1.46(t)[69.6] [b]	2.65(t)[11.7] [c]	5.56	4.48
				1.42(t)[69.4]	2.18(t)[11.7]	4.43	4.40
				1.34(t)[69.6]		4.34	4.26
			meso		2.71 [d]		
		+60	DL/*meso*	1.51(t)	2.46 [e]	5.12	4.42
				1.42(t)		4.33	

[a] Signals show weak multiplet structure in most cases. [b] ^2J(PtH), t = triplet. [c] ^3J(PtH). [d] ^{195}Pt satellites obscured. [e] ^{195}Pt satellites not resolved.

Table 4

^{195}Pt NMR data [a] for the complexes [PtXMe$_3$(BMSF)] and [PtXMe$_3$(BMSEF)]

Complex	Invertomer	%	Chemical shift, δ [b]	^1J(PtSe) (Hz)
1	DL	90.4	1597	–
	meso	9.6	1614	–
2	DL	94.2	1474	–
	meso	5.8	1504	–
3	DL	96.5	1262	–
	meso	3.7	1315	–
4	DL	95.6	1453	231, 339
	meso	4.4	1502	
5	DL	~ 97 [c]	1314	242, 349
	meso	~ 3 [c]	[d]	
6	DL	98.3	1076	251, 367
	meso	1.7	1168	

[a] Complexes **1–3**, CD_2Cl_2 solution −90 °C; complexes **4–6**, $CDCl_3$ solution −40 °C. [b] Relative to Ξ (^{195}Pt) 21.4 MHz. [c] Estimated from ^{1}H spectrum. [d] Not detected.

species on the front and rear faces. Previous studies on analogous palladium(II) and platinum(II) complexes [Fe(C$_5$H$_4$SR)$_2$MX$_2$] (X = Cl, Br) [11] and Group 6 metal complexes [Fe(C$_5$H$_4$ECH$_3$)$_2$M(CO)$_4$] (M = Cr, Mo, W; E = S, Se) [3] have shown clearly that the bridge reversal process is fast on the NMR chemical shift timescale at all accessible temperatures. Therefore, rapid exchange must be envisaged between adjacent structures on the front and rear faces of the cube diagram (Fig. 2), and the observed spectral changes are due solely to chalcogen inversion between bridge-re-

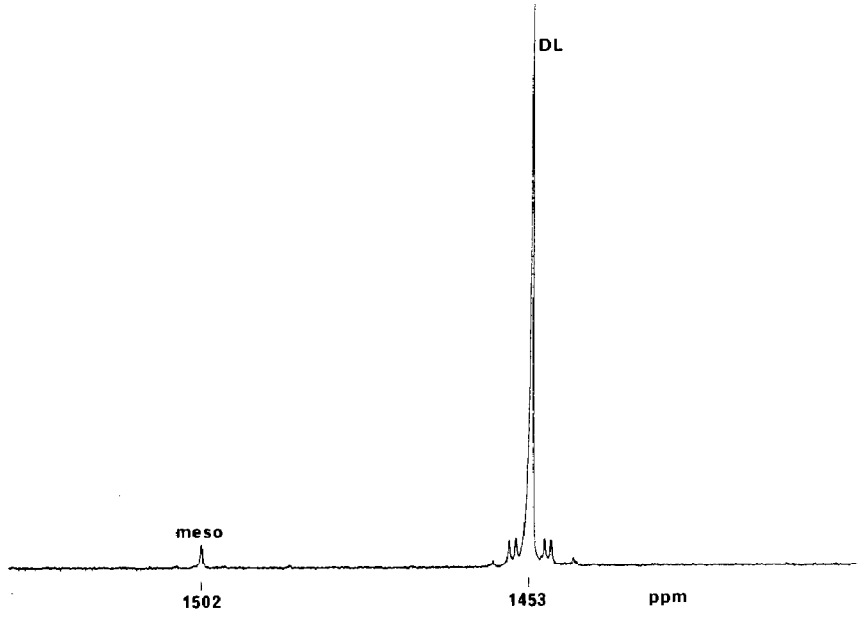

Fig. 1. ^{195}Pt NMR spectrum (−40 °C, $CDCl_3$) of [PtClMe$_3$(BMSEF)] showing the DL-**1** and *meso* species.

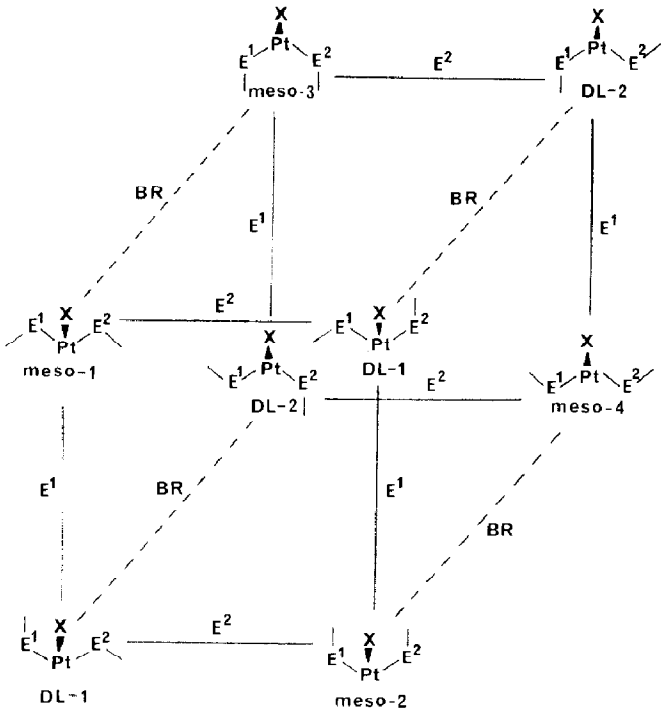

Fig. 2. Graph diagram showing the relationships of the static invertomers of $[PtXMe_3(BMSF)]$ or $[PtXMe_3(BMSEF)]$. BR = bridge reversal, E^1, E^2 = pyramidal E inversion.

versal averaged DL and *meso* species. In the case of the DL species, steric factors between the ferrocenyl chalcogenide ligand and the $PtXMe_3$ moiety favour DL-**1** more than DL-**2** and thus the measured DL shifts are weighted in favour of DL-**1**. In the case of the four *meso* species, the one with the most favourable relationship of E-methyls both towards each other and towards the $PtXMe_3$ moiety would appear to be *meso*-**1**. However, the higher frequency ^{195}Pt shift of the *meso* species relative to DL-**1** favours *meso*-**2** as the detected species, since previous studies of $[PtXMe_3\{MeSe(CH_2)_nSeMe\}]$ ($n = 2$, 3) [12] have shown that *meso* invertomers with Se-methyls *cis* to halogen invariably exhibit a higher frequency ^{195}Pt shift compared to the DL invertomers. If this trend is assumed to be valid in these ferrocenophane complexes, then *meso*-**2** is indicated. In the remainder of the text, the minor solution species of all six complexes will be referred to as *meso*-**2** but it should be recognised that arguments are fairly evenly balanced between *meso*-**1** and *meso*-**2**. Comparison of $^1J(PtSe)$ values between this and the previous work shows clearly that the larger values (339–367 Hz, Table 4) may be attributed to coupling to Se atoms with an attached methyl *cis* to halogen.

Thus, the dynamic NMR exchange problem is confined essentially to the front face of the cube diagram and involves exchange between *meso*-**2** and the DL-**1** pair. However, because of the very low intensities of the *meso*-**2** signals, the subsequent bandshape analysis of the ^1H NMR signals was restricted to the DL-**1** signals, without any loss of accuracy. Scheme 1 below summarises the above arguments.

All the complexes show the same general variable temperature ^1H NMR features, spectral band changes occurring in the ring methine, E-methyl, and Pt-methyl

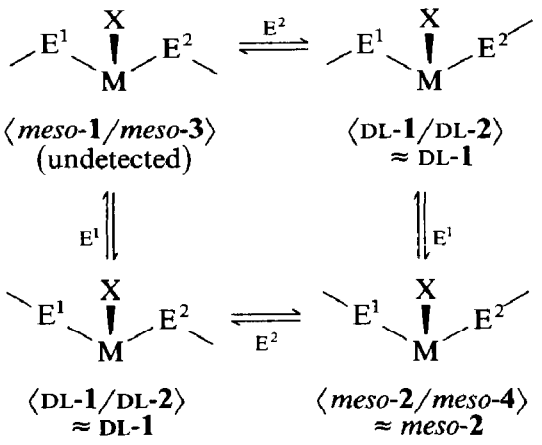

Scheme 1

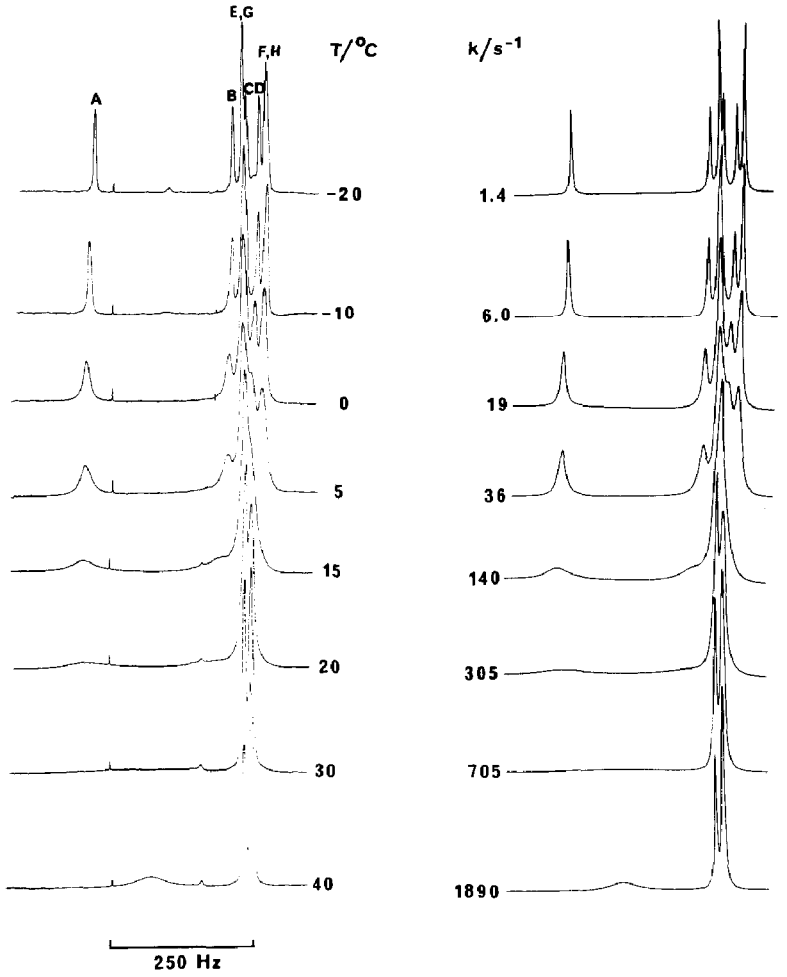

Fig. 3. Variable temperature ^1H NMR spectra of $[PtClMe_3(BMSEF)]$ showing the effects of selenium inversion on the methine proton signals. Computer simulated spectra are shown alongside with the 'best-fit' rate constants. See Fig. 4 for signal labelling.

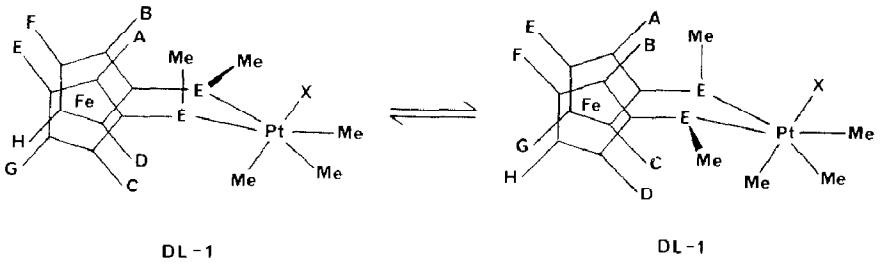

Fig. 4. The effects of chalcogen inversion on the methine proton environments, A–H.

regions. On raising the temperature, the two E-methyl signals coalesced, and the variable number of methine proton signals (depending on the complex) reduced to three signals at high temperatures. The methine regions of the spectra, as exemplified by the spectrum of [$PtClMe_3$(BMSEF)] (Fig. 3), displayed the highest degree of exchange broadening and therefore bandshape analyses were performed on these regions.

The eight methine protons in the DL pair are all distinct and are labelled A–H (Fig. 4). The precise assignment of the methine signals to these eight protons is not straightforward, but fortunately this is not a prerequisite for the bandshape analysis. All that is required are the identities of the exchanging pairs of methine signals. According to Figure 4 these pairs will be A $\rightleftharpoons$ B, C $\rightleftharpoons$ D, E $\rightleftharpoons$ F and G $\rightleftharpoons$ H. However, eight distinct methine signals were not observed for any of the complexes, the maximum number being six, and in some cases fewer (see Tables 2, 3). The exchanges of the methines most remote from the sites of inversion, namely E $\rightleftharpoons$ F and G $\rightleftharpoons$ H could not be distinguished, probably because there was very little difference between the shifts E and G, and between shifts F and H. Also, the chemical shifts of methines C and D were almost identical in the case of the BMSF complexes. The main cause of the exchange broadening was the A $\rightleftharpoons$ B exchange due to the protons closest to the sites of chalcogen inversion. The case of [$PtClMe_3$(BMSEF)] is illustrated in Fig. 3. At low temperatures ($\leqslant -20\,^{\circ}C$) six methine proton signals were detected and assigned as shown to three distinct pairs of exchanging protons. Bandshape analysis was performed on this basis and theoretical spectra matched with experimental spectra in the temperature range -20 to $40\,^{\circ}C$. 'Best-fit' rate constants were deduced, magnitudes varying from 1.4 s^{-1} ($-20\,^{\circ}C$) to 1890 s^{-1} ($40\,^{\circ}C$). At the highest temperature studied ($40\,^{\circ}C$), there was still some residual exchange broadening, particularly in the A $\rightleftharpoons$ B exchange region, but three averaged chemical shifts were clearly detected, implying that a pair of methine protons on each ring (probably E/G and F/H) remained isochronous at all temperatures.

The activation energies of these pyramidal inversions are listed in Table 5. The magnitudes of the $\Delta G^{\ddagger}$(298 K) parameters fall in the narrow ranges 41.7–43.4 kJ mol^{-1} for the sulphur ligand (BMSF) complexes and 58.0–58.8 kJ mol^{-1} for the selenium ligand (BMSEF) complexes. There is, therefore, a negligible halogen influence on the chalcogen inversion barriers. The lower barriers for S inversion compared to Se inversion are in full accord with previous data [1]. The magnitudes of these barriers are somewhat lower than those found in related Pt^{IV} six-membered ring chelate complexes. Three comparisons will suffice, namely [$PtClMe_3$(MeS-

Table 5

Arrhenius and Eyring activation parameters for chalcogen inversion in $[PtXMe_3L]$ (L = BMSF or BMSEF)

Complex	E_a (kJ mol^{-1})	$\log_{10}$ (A/s^{-1})	$\Delta H^{\ddagger}$ (kJ mol^{-1})	$\Delta S^{\ddagger}$ (J K^{-1} mol^{-1})	$\Delta G^{\ddagger}$ (298 K) (kJ mol^{-1})
1	61.5 ± 1.4	16.0 ± 0.3	59.6 ± 1.4	54 ± 6	43.4 ± 0.4
2	65.8 ± 0.2	16.8 ± 0.1	63.8 ± 0.2	70 ± 1	42.97 ± 0.04
3	67.4 ± 1.4	17.3 ± 0.3	65.4 ± 1.4	80 ± 6	41.7 ± 0.4
4	80.2 ± 1.6	16.7 ± 0.3	77.9 ± 1.6	67 ± 6	58.04 ± 0.09
5	73.3 ± 1.7	15.4 ± 0.3	70.9 ± 1.7	41 ± 6	58.65 ± 0.10
6	72.6 ± 1.1	15.2 ± 0.2	70.2 ± 1.1	38 ± 4	58.80 ± 0.05

$(CH_2)_3SMe\}]$ (55.0 kJ mol^{-1}) [13], $[PtClMe_3\{MeSe(CH_2)_3SeMe\}]$ (72.2 kJ mol^{-1}) [13], and $[PtClMe_3(MeSCH_2SCH_2SMe)]$ (55.7, 58.0 kJ mol^{-1}) [14].

The activation entropies, $\Delta S^{\ddagger}$ (Table 5) are noticeably positive as was found in the previous study on the analogous metal tetracarbonyl complexes $[M(CO)_4(BMSF)]$ and $[M(CO)_4(BMSEF)]$ [3]. In that work the positive $\Delta S^{\ddagger}$ values were attributed to the rapid bridge reversal process which accompanies the chalcogen inversion and which contributes to a more highly flexible transition state than that associated with pure pyramidal inversion. We believe a similar argument is equally valid for the present Pt^{IV} complexes.

Previous studies of complexes formed from the trimethylplatinum(IV) halide moiety have identified a fluxional process which usually involves a ligand movement (e.g. 180° rotation) which leads to a loss of distinction between the Pt-methyls *trans* to halide (axial) and *trans* to ligand (equatorial) [1]. We therefore investigated whether a similar fluxion was operating in these ferrocenophane complexes by examining the ^1H NMR spectra of $[PtBrMe_3(BMSF)]$ in the temperature range 20–80 °C (Fig. 5). At the lower temperature, three methine signals were detected in the relative intensity ratio 1/1/2 (see earlier) and two Pt-methyl signals in the intensity ratio 2/1. On warming the $C_2D_2Cl_4$ solution, loss of distinction between the Pt-methyls was achieved by ca. 50 °C, and the lower intensity pair of methine signals broadened, coalesced at ca. 75 °C and then sharpened. These changes provide clear evidence that Pt-methyl scrambling is occurring accompanied by 180° 'pancake' rotations of the BMSF or BMSEF ligand about the axis containing the Fe and Pt atoms (see Fig. 4). Such a fluxion removes distinction between the two inversion-averaged methine environments ⟨AB⟩ and ⟨CD⟩. The other methines on each ring E, G and F, H were already indistinguishable due to their remoteness from the inverting chalcogens and their signal was therefore unaffected by the high temperature fluxion. These observations also confirm the correctness of the low temperature spectral assignments of the methine region, and lend support to a concerted ligand rotation/Pt-methyl scrambling fluxion occurring as in previous Pt^{IV} complexes [1].

No activation energy data were measured for this Pt-methyl fluxion but qualitative observations of the exchange-broadened proton spectra suggest that the energy barrier will be in the region of 80–90 kJ mol^{-1} as found previously for the complexes $[PtXMe_3L]$ (L = sulphur or selenium chelate ligands) [1].

This work shows that when comparisons are made between the present ferrocenophane complexes and the dithio- and diseleno-ether complexes of $PtXMe_3$,

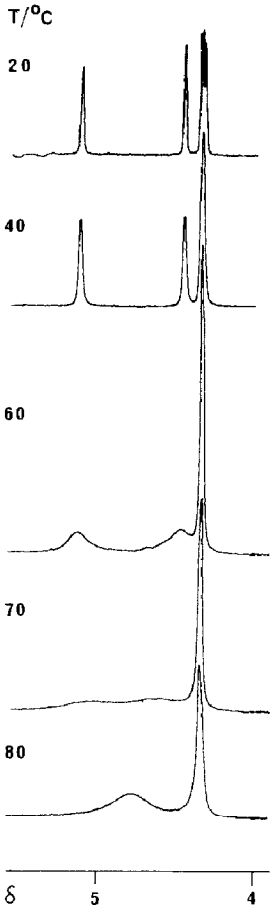

Fig. 5. Above-ambient temperature ^{1}H spectrum of the methine signals of [$PtBrMe_3$(BMSF)] showing the high temperature fluxionality.

there are distinct differences in the preferred low temperature solution invertomers and in the energies of chalcogen inversion, the latter being appreciably lower in the ferrocenophane complexes, probably as a result of the greater flexibility of the ferrocenyl chalcogenide ligand ring.

Acknowledgement

We thank the University of Exeter for a Frank Southerden Scholarship to N.J.L., and Dr. David Stephenson for recording the ^{195}Pt NMR spectra.

References

1 E.W. Abel, S.K. Bhargava and K.G. Orrell, Prog. Inorg. Chem., 32 (1984) 1.
2 K.G. Orrell and V. Šik, Ann. Rep. NMR Spectrosc., 19 (1987) 79.
3 E.W. Abel, N.J. Long, K.G. Orrell, A.G. Osborne, V. Šik, P.A. Bates and M.B. Hursthouse, J. Organomet. Chem., 367 (1989) 275.
4 D.F. Shriver, Manipulation of air-sensitive compounds, McGraw-Hill, New York, 1969.
5 J.C. Baldwin and W.C. Kaska, Inorg. Chem., 14 (1975) 2020.
6 D.E. Clegg and J.R. Hall, J. Organomet. Chem., 22 (1970) 491.

7 D.E. Clegg and J.R. Hall, Spectrochim. Acta, 21 (1965) 357.
8 B. McCulloch, D.L. Ward, J.D. Woolins and C.H. Brubaker, Jr., Organometallics, 4 (1985) 1425.
9 D.A. Kleier and G. Binsch, J. Magn. Reson., 3 (1970) 146.
10 D.A. Kleier and G. Binsch, DNMR3 Program 165, Quantum Chemistry Program Exchange, Indiana University 1970.
11 K.G. Orrell, V. Šik, C.H. Brubaker, Jr., and B. McCulloch, J. Organomet. Chem., 276 (1984) 267.
12 E.W. Abel, K.G. Orrell, and A.W.G. Platt, J. Chem. Soc., Dalton Trans., (1983) 2345.
13 E.W. Abel, A.R. Khan, K. Kite, K.G. Orrell and V. Šik, J. Chem. Soc., Dalton Trans., (1980) 1175.
14 E.W. Abel, M.Z.A. Chowdhury, K.G. Orrell and V. Šik, J. Organomet. Chem., 258 (1983) 109.